Publications of the Ray W. Herrick Laboratories   School of Mechanical Engineering

8-2023

Modeling of Sound Radiation from a Loaded Rolling Tire

Won Hong Choi
Samsung Electronics, romeowonhong@gmail.com

J Stuart Bolton
Purdue University, bolton@purdue.edu

Modeling of Sound Radiation from a Loaded Rolling Tire

Won Hong Choi, J. Stuart Bolton

Purdue University

Ray W. Herrick Labs, 177 Russell Street, West Lafayette, IN 47907

Contents

Introduction

1. **Reduction of tire/road noise** is an important issue for EV vehicles
   - Powertrain noise is eliminated for EV vehicles
   - A driver becomes more sensitive to tire/road noise

2. Tire/road noise is also a key contributor to a pass-by noise
   - Traffic noise level allowed in regulations is lowered (e.g., EU, Asia)
   - **Development of a low-noise tire** and pavement enhancement are required

Tire noise in EV vehicle (Parmer [1]).

The dominance of tire noise in pass-by noise (Bernhard [2]).
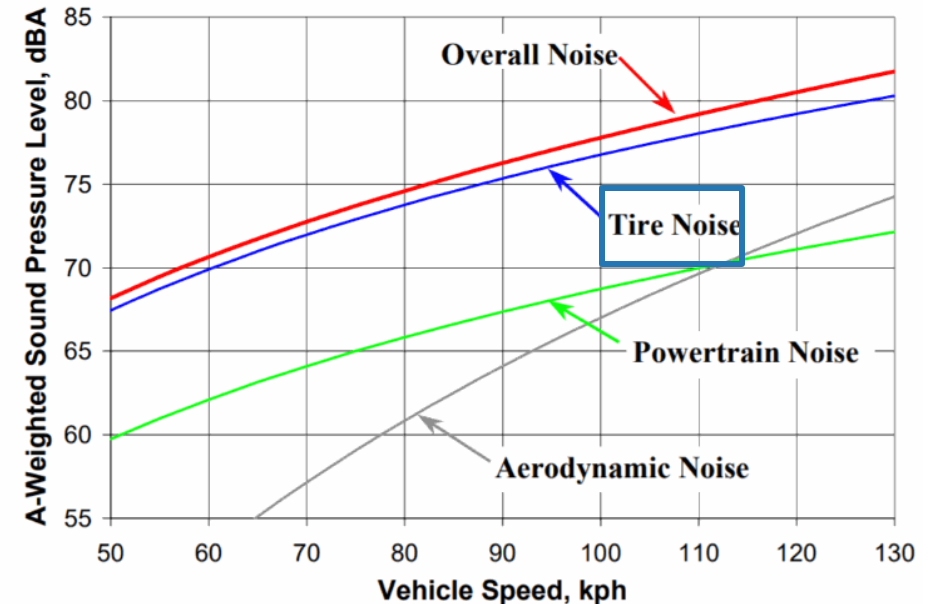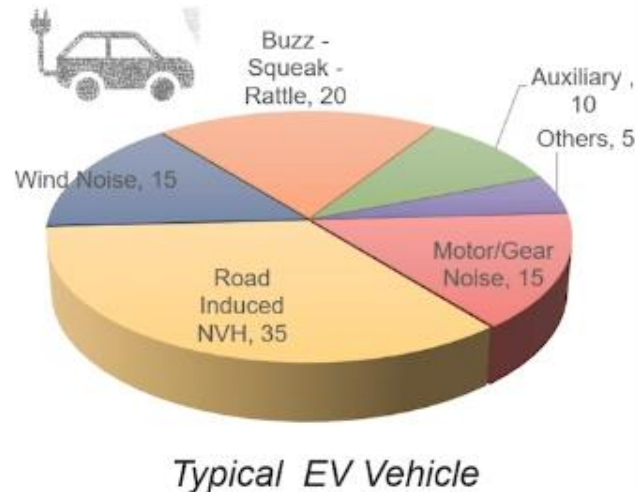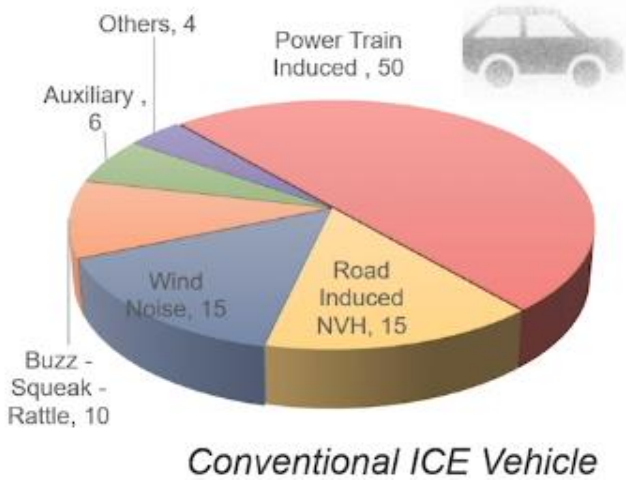
Frequency split in the air-cavity noise

1. **The fundamental air-cavity mode** is an acoustic resonance mode between 180 Hz and 250 Hz

2. It contributes to **the increased spindle force and cabin noise** due to the large net displacement

3. **The frequency split** in the fundamental air-cavity mode is caused by **a static load** and **Doppler shift**
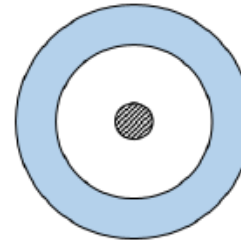
Cavity noise at 200 Hz (Warped perception[3]).
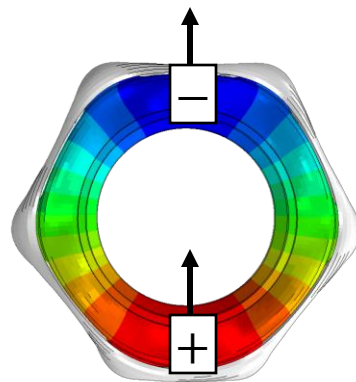
Acoustic mode (n=1st).

The **unloaded static** tire when excited will show just one tire cavity mode

Upon loading the tire cavity mode splits as fore/aft and vertical cavity mode (primary cavity mode)
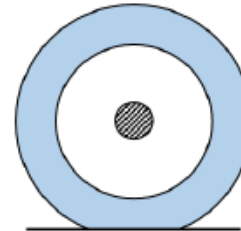
As the **tire starts spinning** the frequencies further change as **measured by a stationary sensor** due to Doppler Effect

$$f = \frac{c}{2\pi R}$$

Deformed

$$f_{H,V} = \frac{c}{L_c \pm (1-m)l_{cp}}$$

Rolling

$$f_{1,2} = f_{H,V} + \frac{c \pm v}{L_c}$$
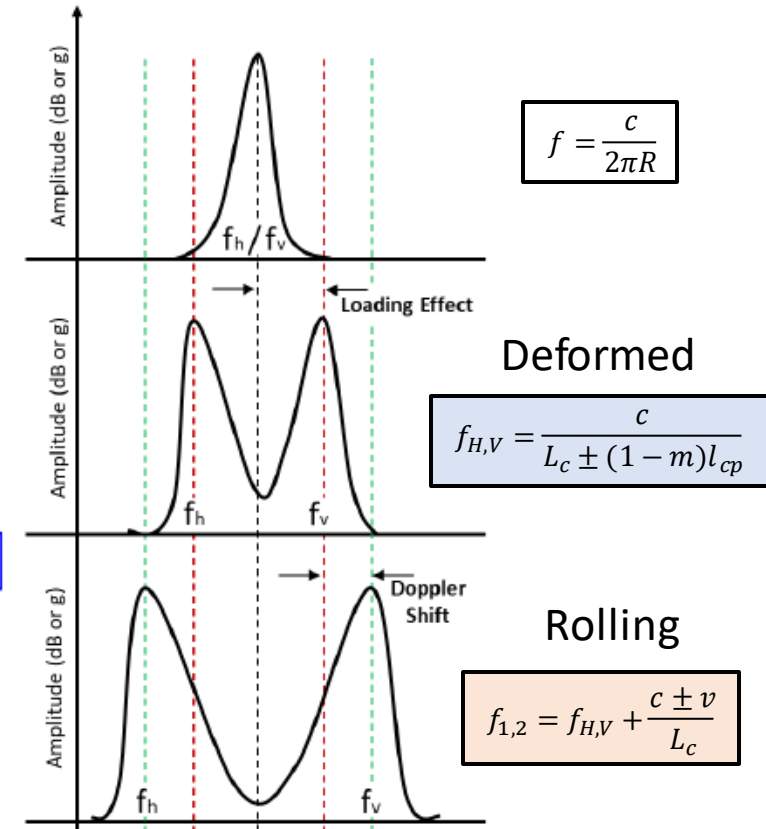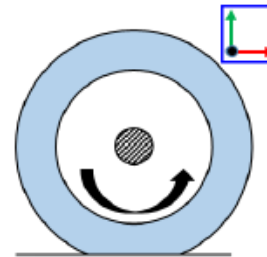
The evolution of frequency split (Patil[4]).

Previous Study

1. The frequency split phenomenon was investigated both numerically and experimentally

2. Correlation between FE simulation and experiment was achieved for force amplification by the split phenomenon

3. **Next, the relation between resultant surface vibration and the exterior noise needs to be studied**

Force amplification due to the frequency split in air-cavity mode [6].
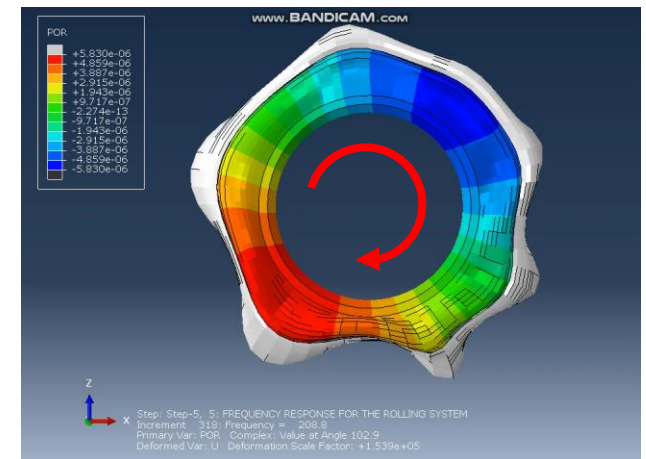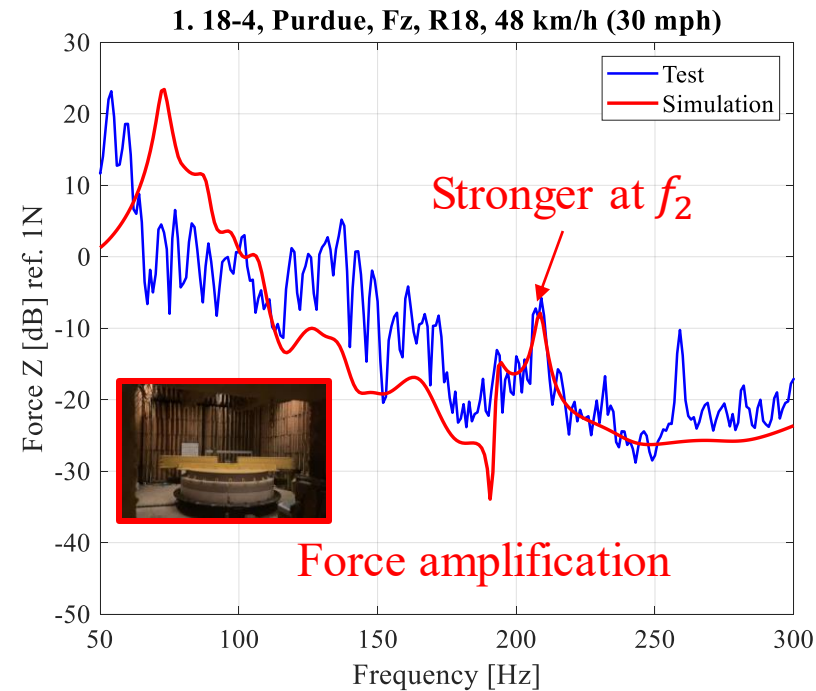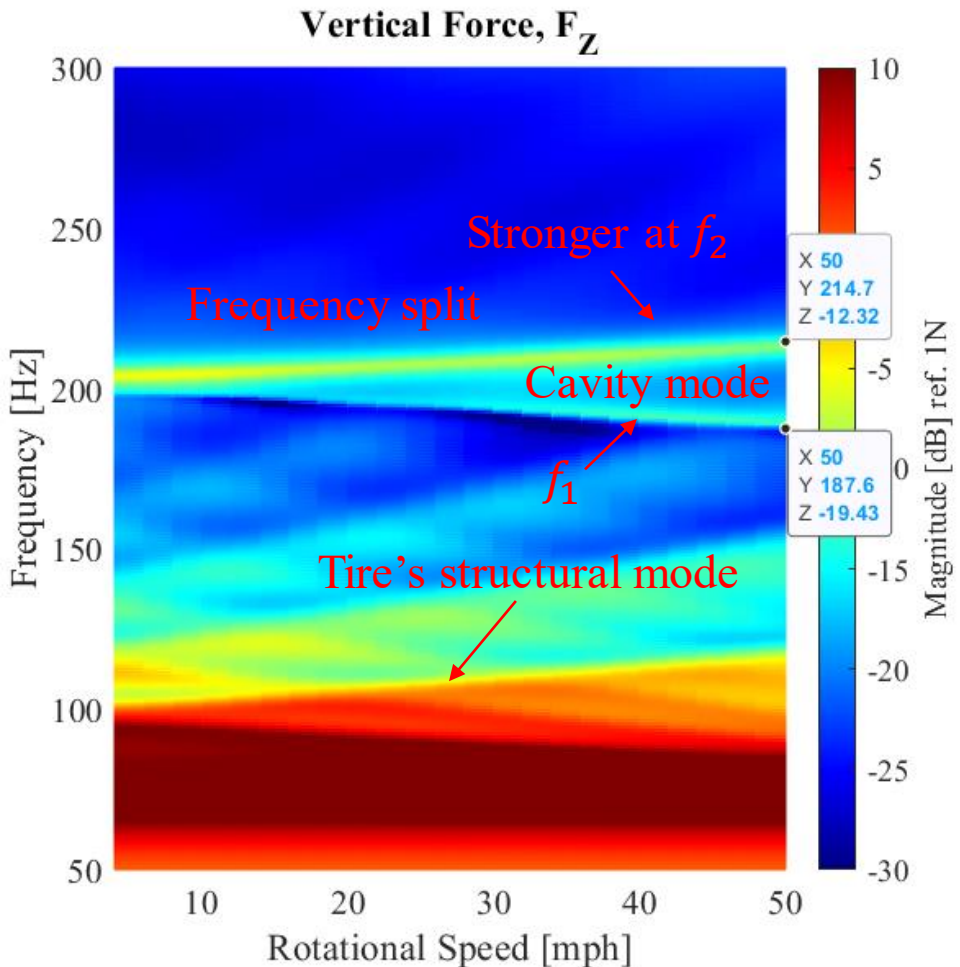
Acoustical and structural mode shape for rolling tire.

BEM (Boundary Element Method)

1. **The boundary element method** is a numerical procedure to solve partial differential equations relating to acoustical and other physical problems

2. From the transfer function between the surface boundary of a closed volume and the acoustic field at a certain point, it is possible to **calculate the sound pressure surrounding the object**

BEM Mesh in Human Face[5].

BEM domain[5].
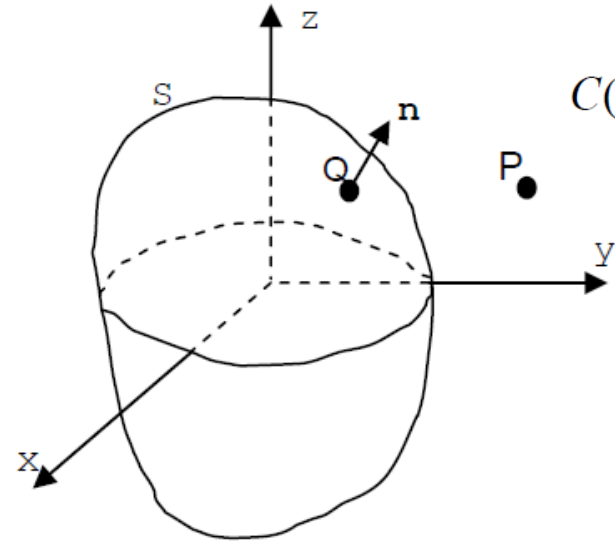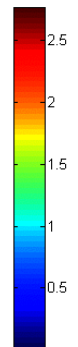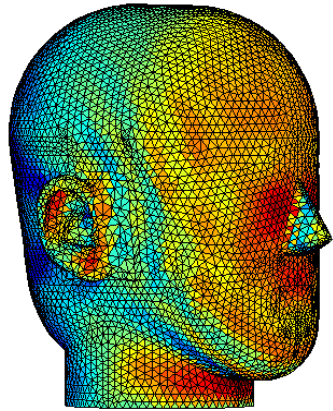
==Helmholtz equation in a generic domain==

$$C(P)p(P) = \int_S \left(\frac{\partial G}{\partial n} p(Q) + ikz_0 v(Q)G \right) dS + 4\pi p^I(P) \qquad (1)$$

==A discretized version for Matrix computation==

$$Cp = Ap_s + ikz_0 Bv_n + 4\pi P^I \qquad (1)$$

where p_s and v_n denote the pressure and normal velocity at the nodes of the surface mesh and matrices A and B include integrals of the kernel functions. C represents exterior solid angle.

Conversion from FEM to BEM (OpenBEM[5])

1. **3D surface meshes** were created by importing a FE model from Abaqus 2020, consisting of treadband, sidewall, and rim, and the ground surface was set to be zero in the vertical direction

2. The import required manual conversion between the **Abaqus** format and the **GMSH** (Open 3D finite mesh generator) format used in the **OpenBEM code**

FE Model (Abaqus)   **R18**   Surface Mesh (GMSH)

Treadband
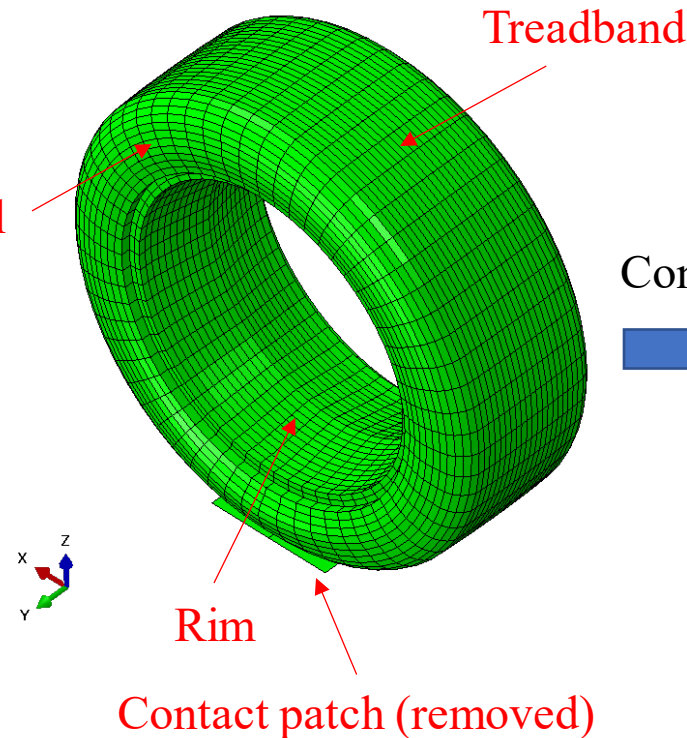
Sidewall

Convert

Rim
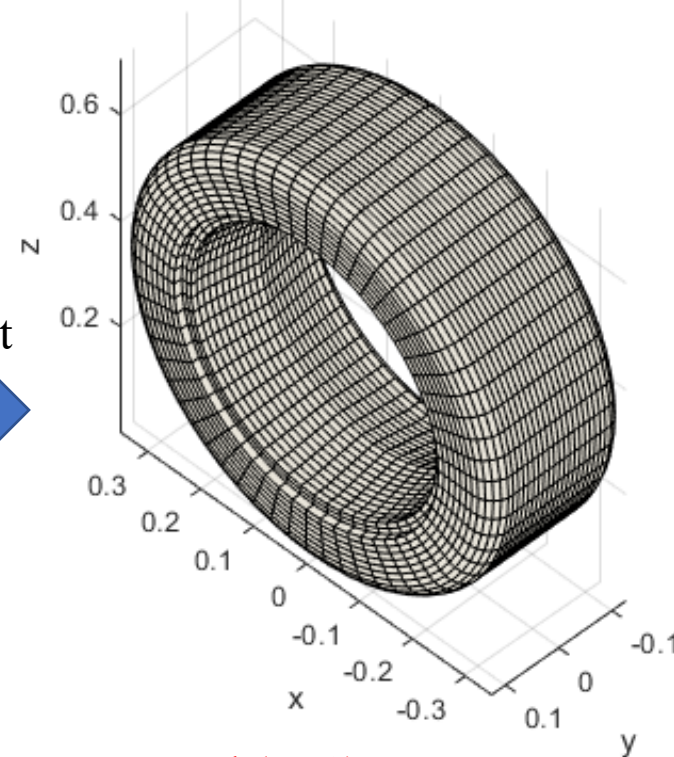
Contact patch (removed)   Ground (Z=0)

Conversion from FEM to BEM (OpenBEM[5])

1. **3D surface meshes** were created by importing a FE model from Abaqus 2020, consisting of treadband, sidewall, and rim, and the ground surface was set to be zero in the vertical direction

2. The import required manual conversion between the **Abaqus** format and the **GMSH** (Open 3D finite mesh generator) format used in the **OpenBEM code**

FE Model (Abaqus)   **R18**   Surface Mesh (GMSH)

Simulated tires

#	ID	Spec	Inflation [psi]	Load [lbs]	Mass [Kg]
1	R18	235/50/R18	35	1245	12.7
2	R19	255/40/R19	32	1073	13.3

Rim

Contact patch (removed)   Ground (Z=0)
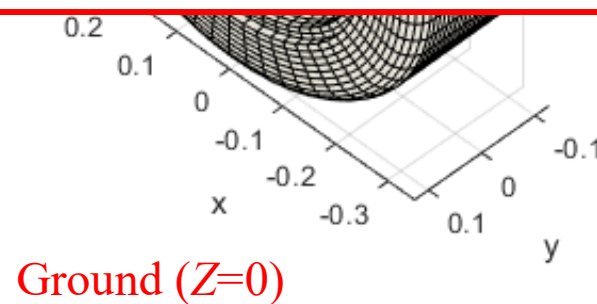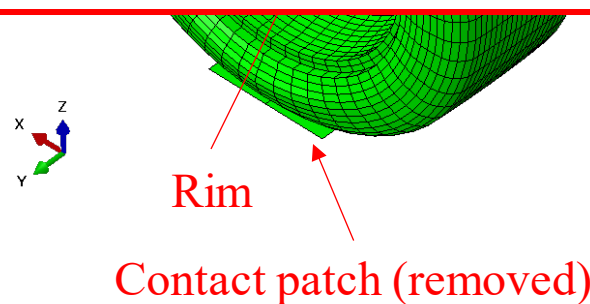
Simulation Procedure (1/3)

1. Previously, it was verified that **the frequency split affects force amplification** near 200 Hz at the hub

2. **Sound radiation pattern at the two split frequencies** was mainly investigated

Horizontal Force, F$_X$ R19 **Vertical Force, F$_Z$**

(a) Spindle forces at the hub [6] (b)
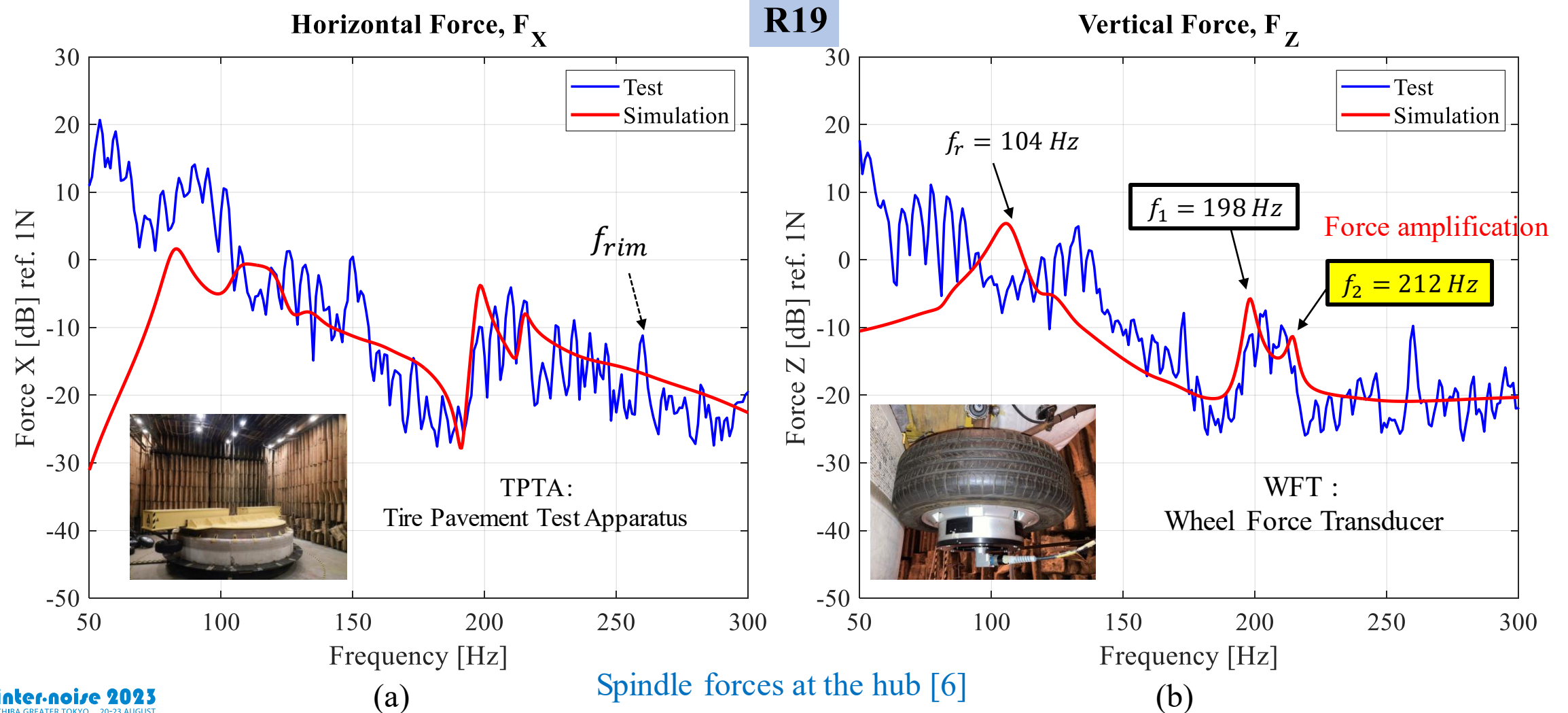
Simulated Procedure (2/3)

1. **Normal surface velocities** (V_n) in a cylindrical coordinate system were imported from simulation results in **Abaqus** at a single frequency of interest (i.e., one of the acoustic cavity mode split frequencies)

2. The velocities were utilized as the input field for Eq. (1) since **there was no external incident pressure (P^I)**

3. A distribution of the surface pressure (P_s) was found by assuming the above equation to be **homogeneous**

Treadband
v_n[m/s]

Sidewall
v_n[m/s]

Overlapped

Surface velocity (cylindrical)

Body nr. 1

Plot : Real{v_n}[m/s]

R19, V=0 mph, f_2=210 Hz

FE Model (Abaqus)

Surface Mesh (BEM)
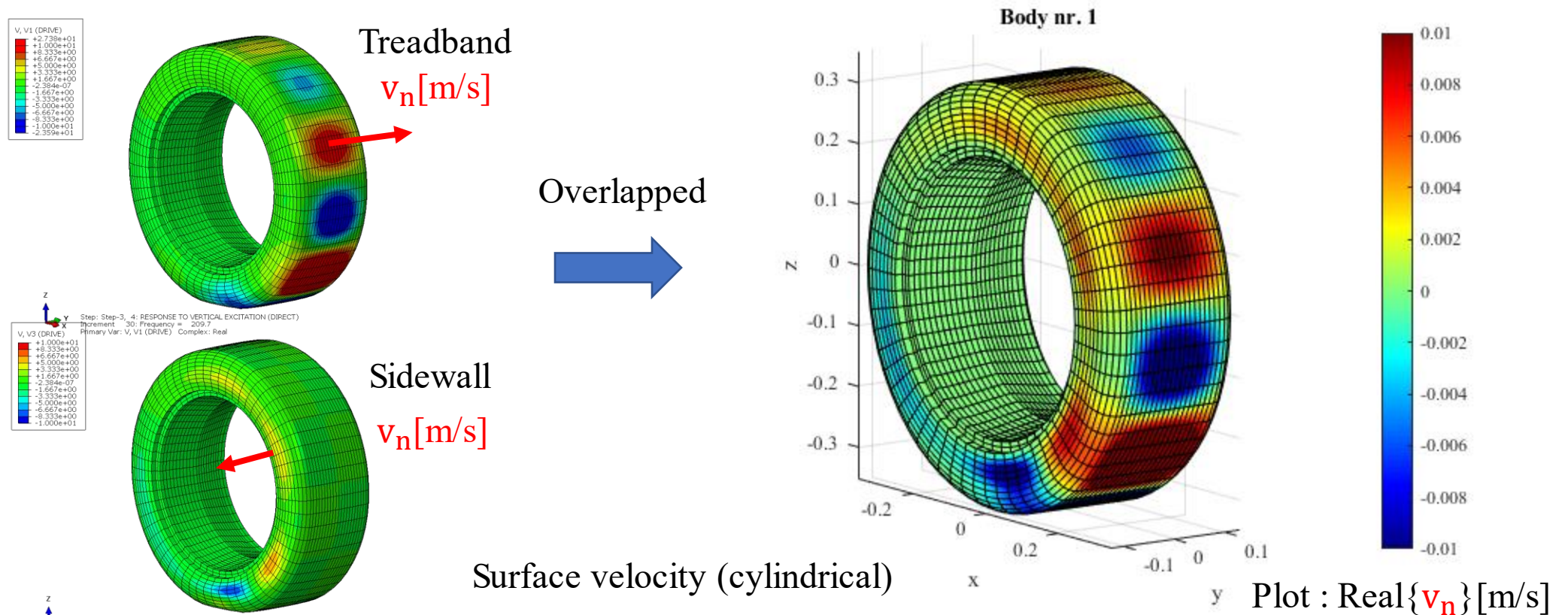
Simulated Procedure (3/3)

1. The **surface pressure** (P_S) was calculated from the **Helmholtz equation**. Then **the acoustic pressure** (P_F) at any distance can be calculated, along with information about the matrices, A, B, and C. **The sound field** radiated by the tire could then be plotted as a function of **radius** and **angle** at the field points of interest

Surface pressure (calculated)
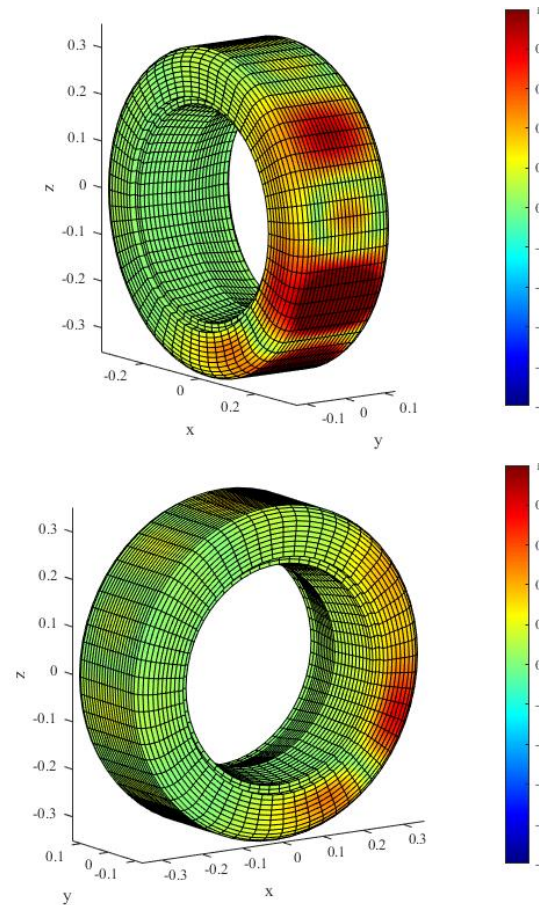
R19, V=0 mph, f_2=210 Hz

Upper side (interested)

r=2.7 [m]

Z=0 (ground)

Plot : Real$\{p_s\}$[Pa]
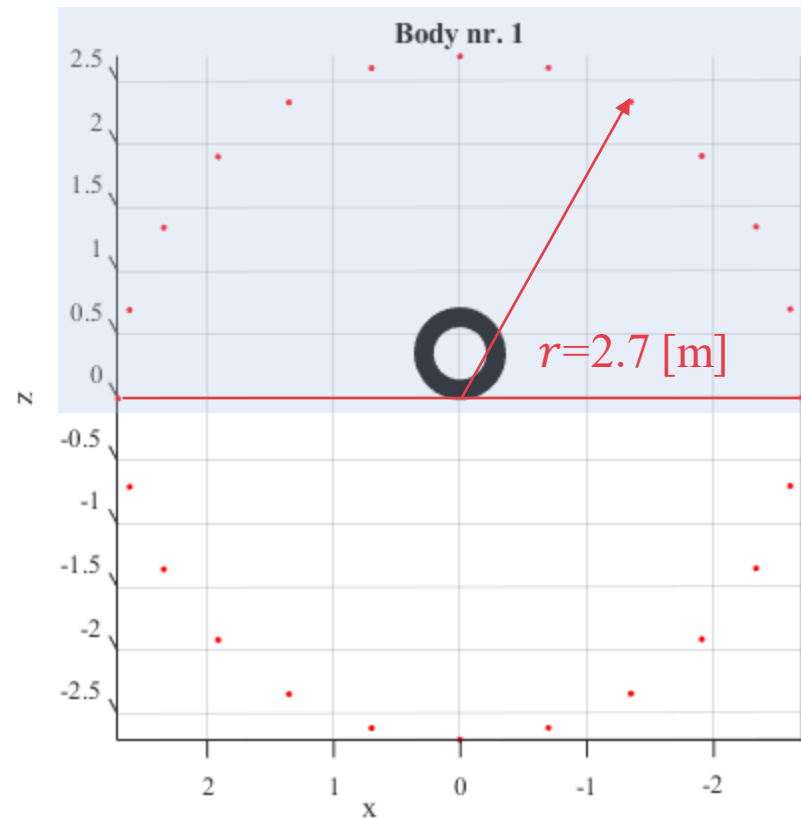
Non-Rotating Tire : Verification

1. To verify the reliability of the BEM analysis, **the simple case of a non-deformed tire** placed on reflecting ground without rotation was compared with **the previous experimental results** obtained by using a circular array of six, half-inch microphones during a drop test by Choi and Bolton [7]

2. It was predicted that **the sound radiation pattern** for a single non-rotating tire had **a quadrupole-like shape** at the vertical cavity mode resonance frequency

Simulation (BEM, R18, Free and Reflected)
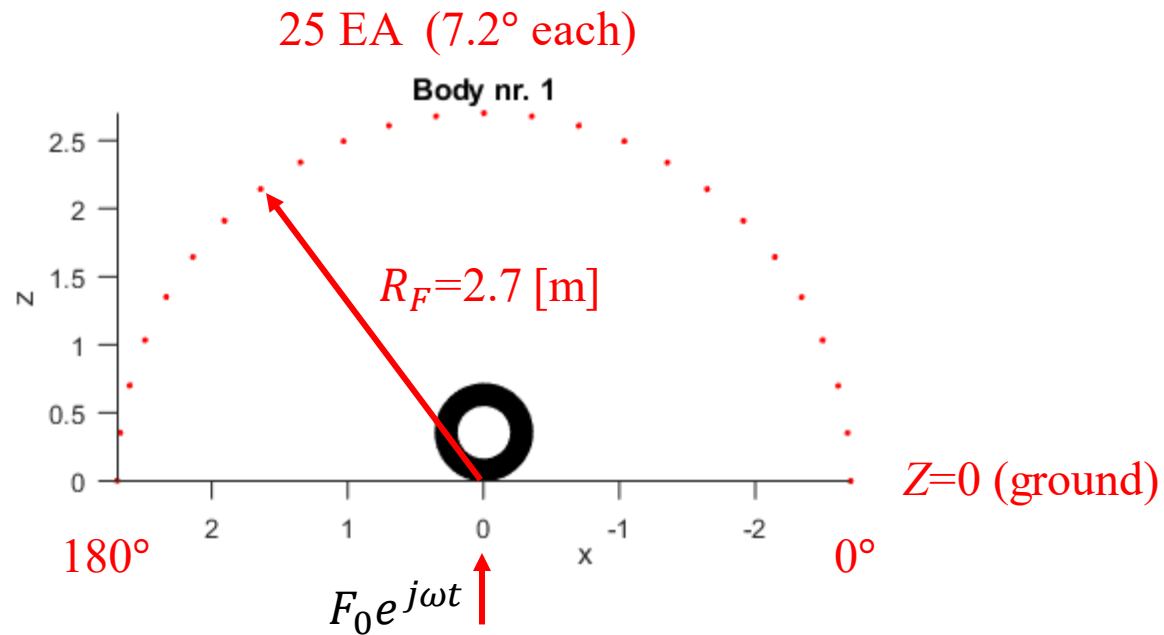
Test (Drop, R14, Reflected)

25 EA (7.2° each)

6EA (15° each)

R_F=2.7 [m]

R_F=2.7 [m]

Z=0 (ground)

180°

0°

$F_0 e^{j\omega t}$
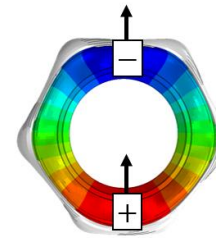
One bounce
(h=0.1m)

Non-Rotating Tire : Verification

1. The radiation pattern from the BEM simulation was changed **from dipole to quadrupole-like** when the **reflecting boundary condition**, image source, on the ground was applied

2. The sound radiation pattern shows a quadrupole shape where the maximum level was measured as 54 [dB], indicating that **the maximum SPL level is in good agreement** between these two results, verifying the **reliability of the BEM analysis** regarding the tire's sound radiation for the simplest case

Simulation (BEM, R18, 208 Hz, Free)   Simulation (BEM, R18, 208 Hz, Reflected)   Test (Drop, R14, 212 Hz, Reflected)
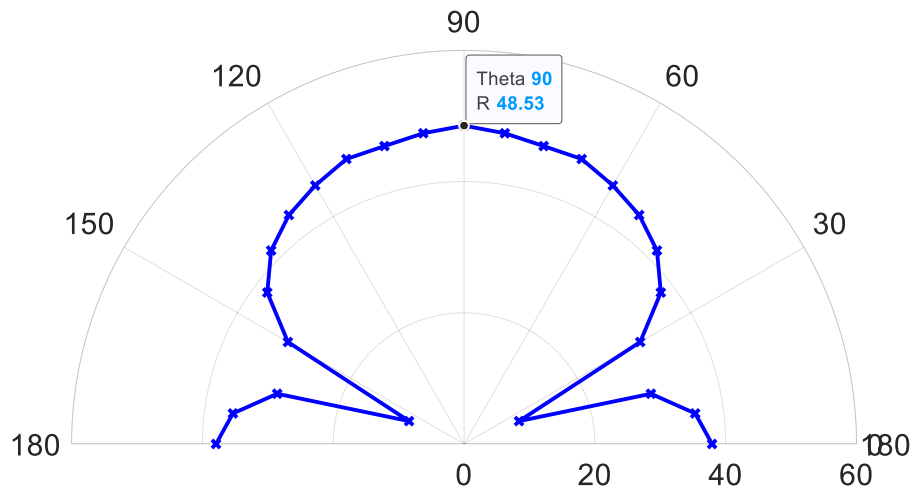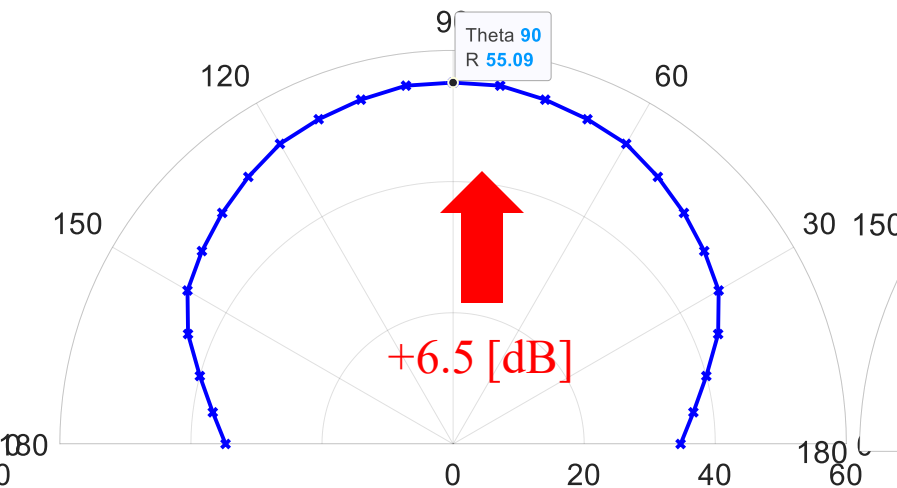
Max=48.5 [dB]   Max=55 [dB], +6.5 [dB]   Max=54 [dB]
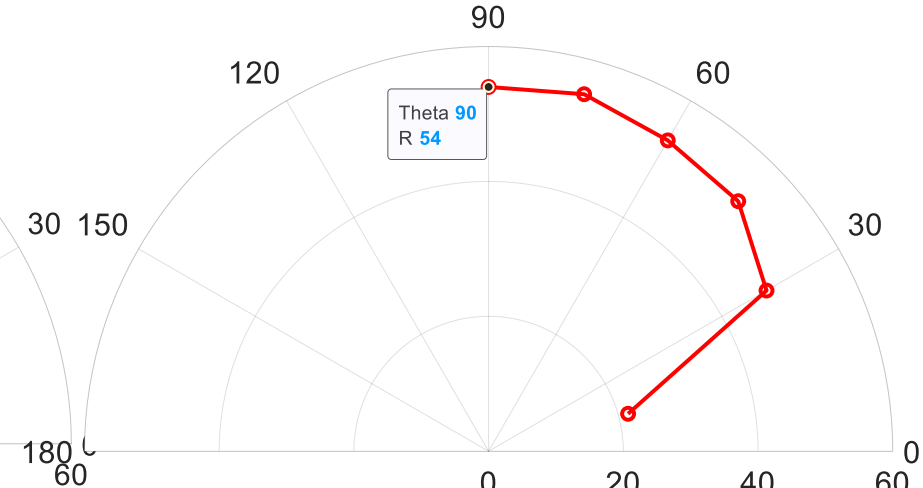
(a)   (b)   (c)

Non-Rotating Tire : Verification

1. It is found that the comparison of the sound radiation map for a full circle between **the BEM simulation and the quadrupole analytical model** for a tire placed on a reflecting ground where these two models are consistent with each other as the strength of the acoustic source was tuned

SPL [dB], Reflected, f=208Hz

R18

Z=0 (ground)

Original

Image

$Q = 0.8\text{e-}04\ [\text{m}^3/\text{s}]$

Analytical solution
(Linear quadrupole)
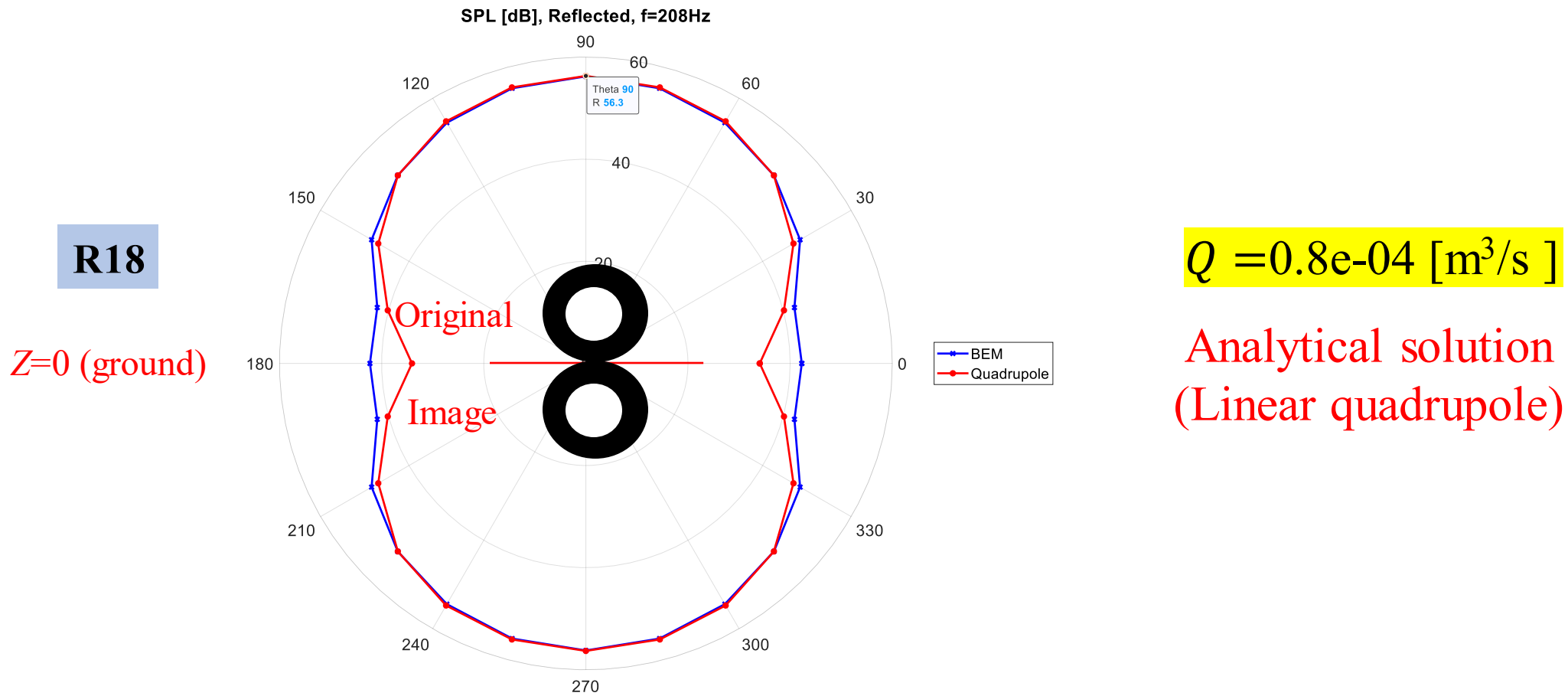
$$P(r,\theta) = \frac{j\rho ckQ}{4\pi r_1} \cdot e^{-jkr_1} - \frac{j\rho ckQ}{4\pi r_2} \cdot e^{-jkr_2} - \frac{j\rho ckQ}{4\pi r_3} \cdot e^{-jkr_3} + \frac{j\rho ckQ}{4\pi r_4} \cdot e^{-jkr_4}$$

Rolling Tire : Free vs. Reflecting Ground

1. The SPL level and directivity for the R19 tire was calculated both in free-field and reflecting conditions to **highlight the effect of reflection** at the secondary split

2. The contribution of the reflection diminishes as the tire **rolls**

due to the rotation when **surface velocity is more evenly distributed** around the tire's circumference

V [mph]	Mean, SPL [dB] Free	Mean, SPL [dB] Refl
0	58.0	63.2 [+5.2]
30	60.2	60.7 [+0.5]

R19

SPL [dB], f_2=210Hz

Theta **120** R **63.29**

Theta **120** R **50.48**

$F_0 e^{j\omega t}$

0 mph, $f_2 = 210\ Hz$

(a)

Mean SPL : 30°~150°

SPL [dB], f_2=214Hz

Theta **120** R **62.84**

Theta **120** R **61.2**

free
refl

$Z=0$ (ground)

$F_0 e^{j\omega t}$

30 mph, $f_2 = 214\ Hz$

(b)
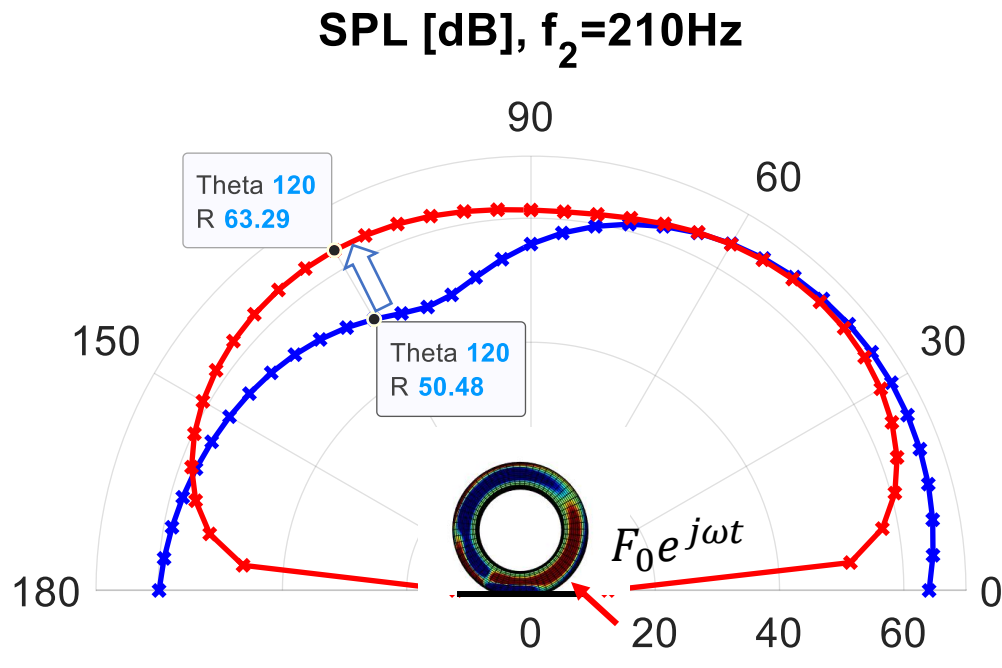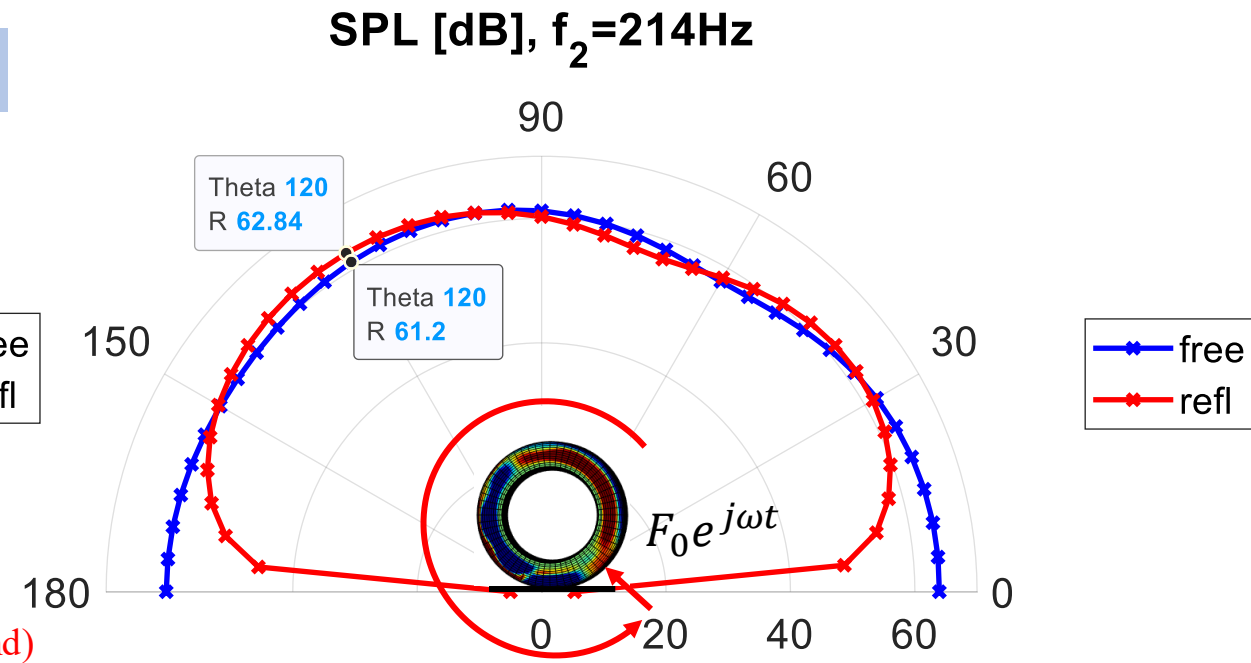
Rolling Tire : The effect of speed on SPL

1. The SPL level reached **the maximum** not at 30 mph, but at **10 mph** as **the strength of coupling** between acoustic mode and structural response is largely dependent on **the rotation speed** while the second split frequency moved farther away at the increased speeds.

Mean SPL : 30°~150°

SPL [dB]

Max. 65 [dB]

Theta **60**
R **65.09**

R19

Legend:
- 0
- 10
- 20
- 30

$F_0 e^{j\omega t}$

Counterclockwise
(rotation in Abaqus)
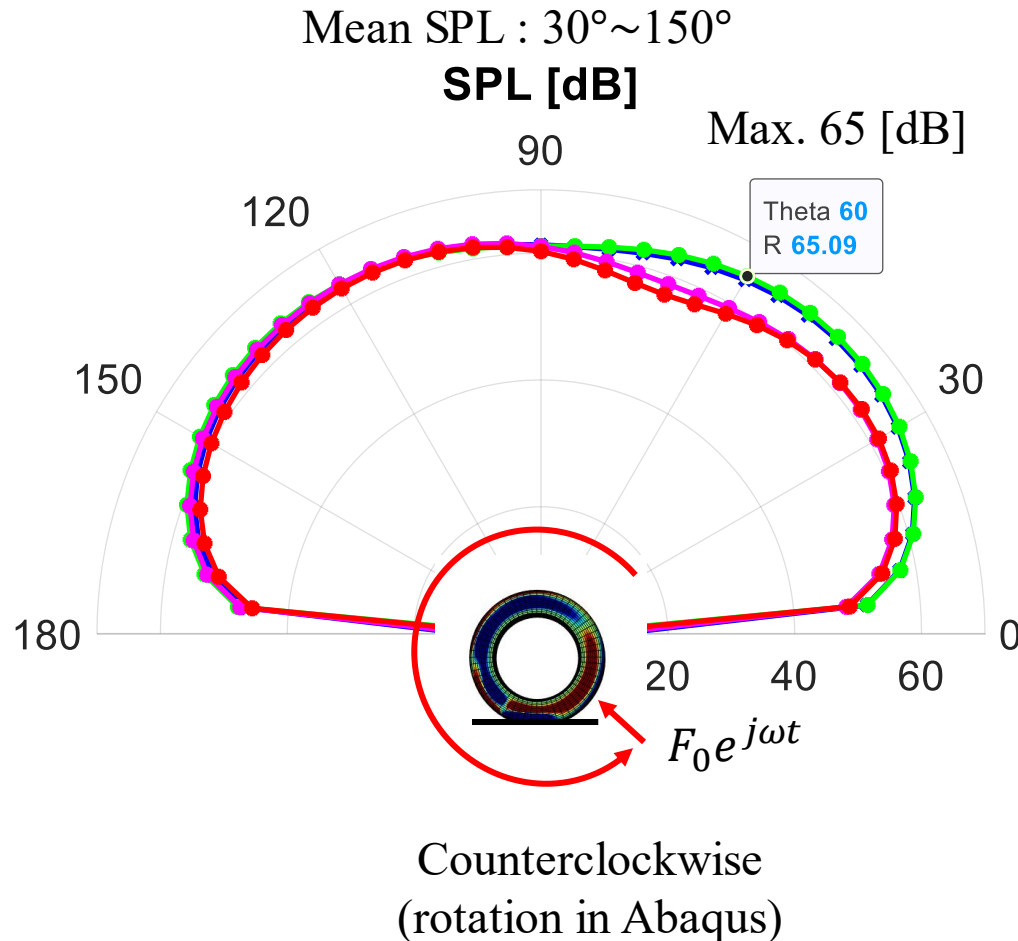
0 mph, $f_2 = 210\ Hz$
10 mph, $f_2 = 212\ Hz$
20 mph, $f_2 = 212\ Hz$
30 mph, $f_2 = 214\ Hz$

Ω [mph]	Mean, SPL [dB]
0	63.2
10	63.6
20	61.5
30	60.7

Rolling Tire : Relation between SPL and Distance

1. **The influence of distance** on the SPL level was also investigated at R_F, $0.5R_F$, and $0.3R_F$
2. The SPL level was investigated for both **free-field** and **reflecting ground**

Free   R19, **V**=0 mph, $f_2 = 210\ Hz$ Reflected

(a) R_F=2.7 [m]   (b)
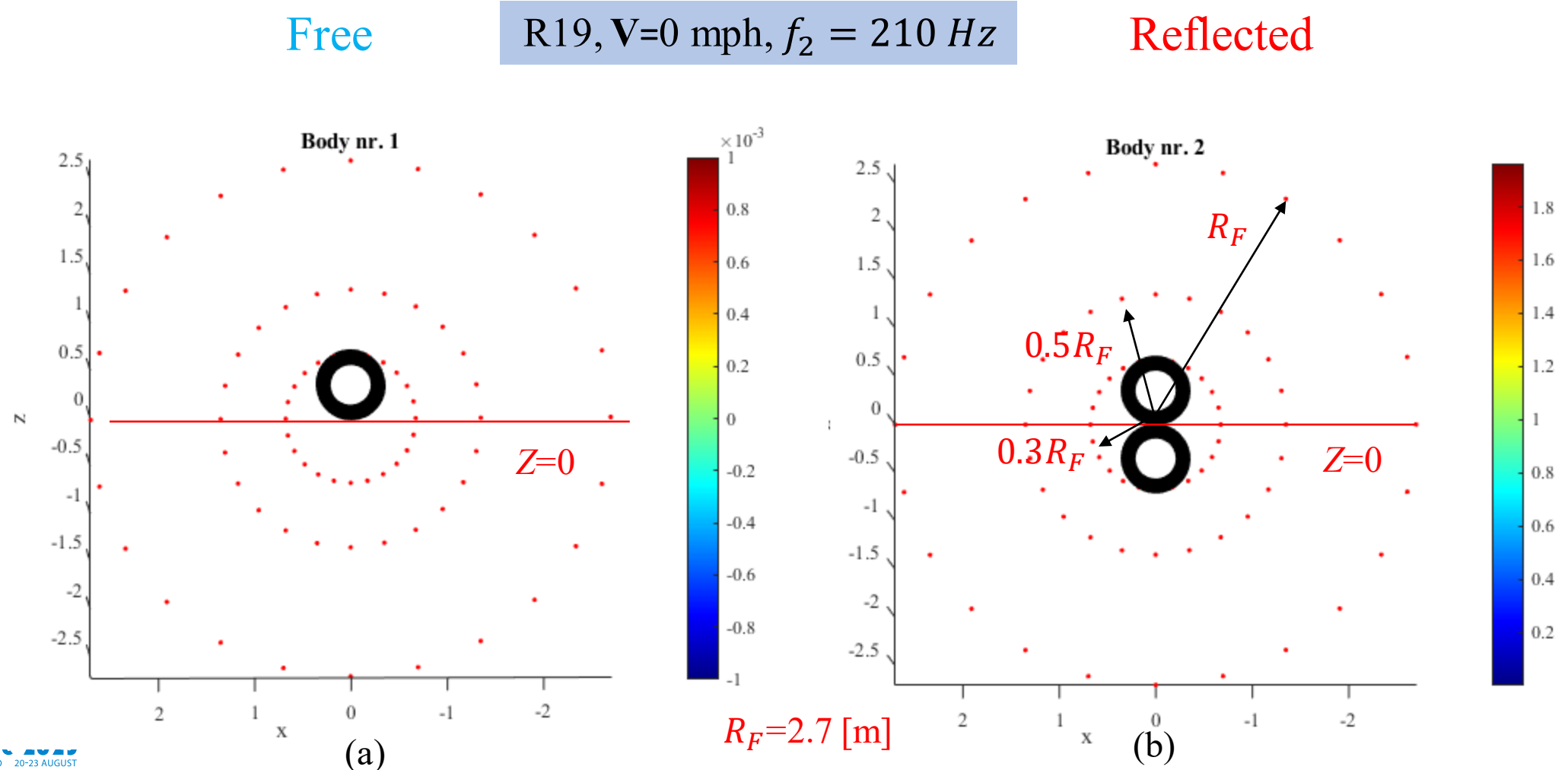
Rolling Tire : Relation between SPL and Distance

1. A doubling effect was clearly observed as the distance was decreased by half, with an increased level of 6~7 [dB] similar to the expected 6 [dB]

Free

R19, **V**=0 mph, $f_2 = 210\ Hz$

Reflected

SPL [dB], f_2=210Hz

Theta **30** R **79.69**

Theta **30** R **73.97**

Theta **30** R **66.97**

R_F

0.5*R_F

0.3*R_F

SPL [dB], f_2=210Hz

Theta **30** R **78.12**

Theta **30** R **72.18**

Theta **30** R **65**

R_F

0.5*R_F
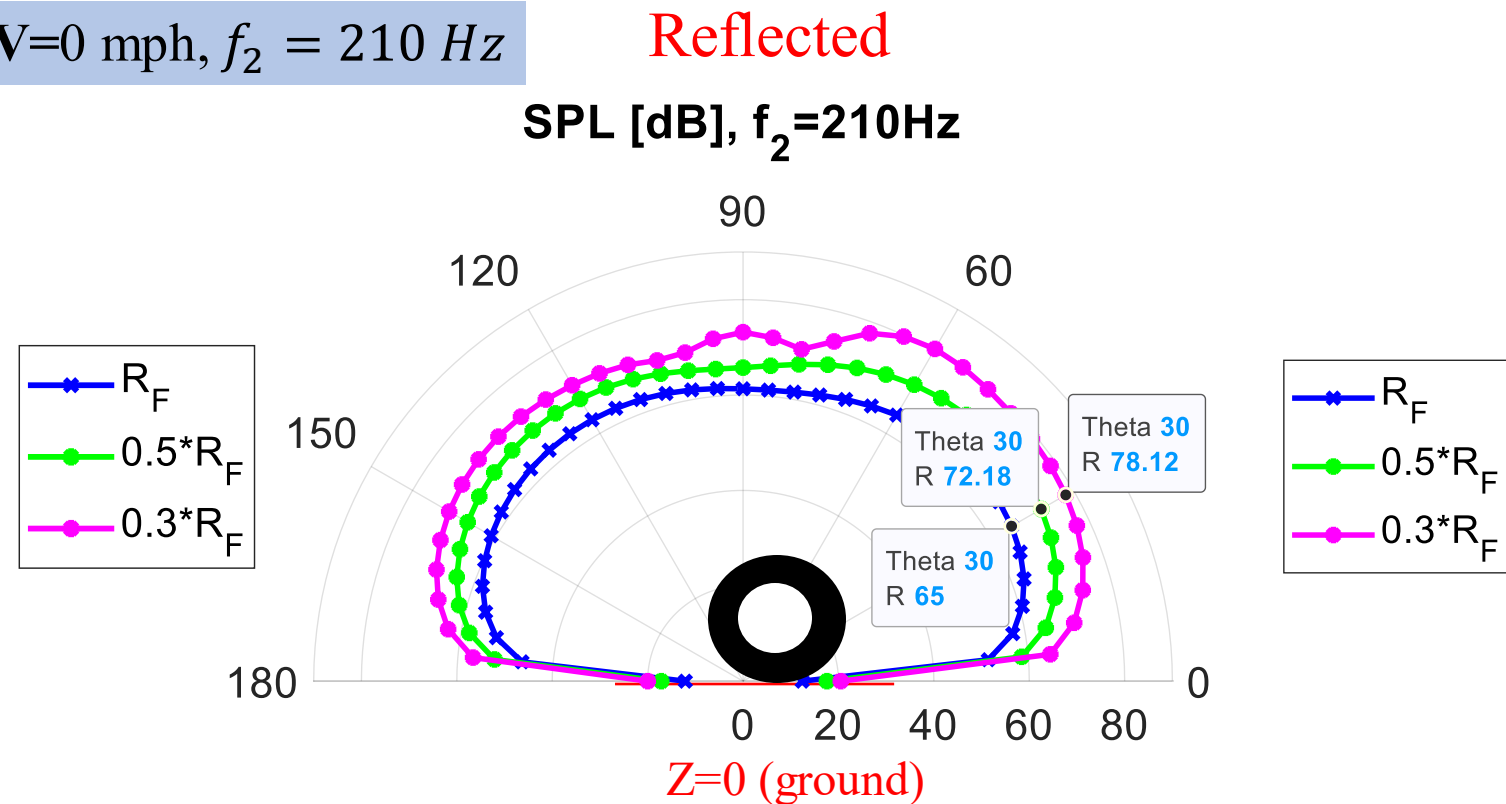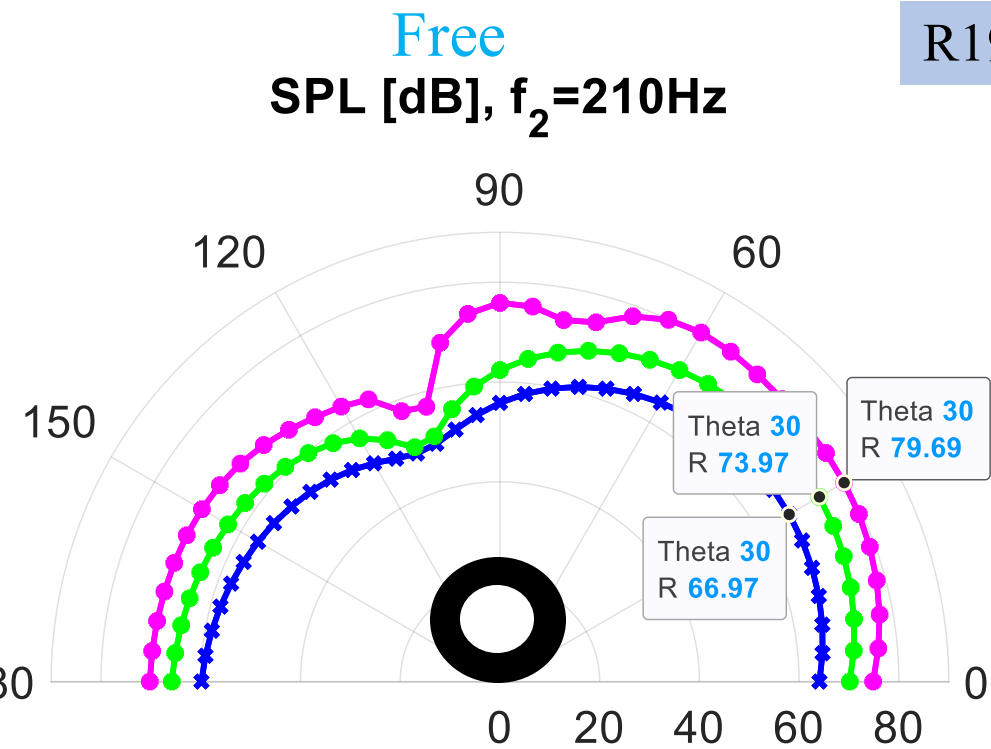
0.3*R_F

Z=0 (ground)

ΔSPL=7 [dB] $R_F \rightarrow 0.5R_F$ ΔSPL=7 [dB]

ΔSPL=6 [dB] $0.5R_F \rightarrow 0.3R_F$ ΔSPL=6 [dB]

cf. +6 [dB] for doubling

Rolling Tire : Sound Map

1. **The entire sound mapping** in the upper hemisphere surrounding a pair of two tires (original and image source due to the reflecting ground) both at 0 mph and 30 mph in terms of **the second split frequency**

2. As expected, **the rotational speed breaks a symmetric feature** of the SPL level since a normal surface velocity as an input variable becomes unsymmetric when the tire is in a rolling condition. However, the maximum level remains around 65 [dB]

Max. 65 [dB]

R19

(a) 0 mph   (b) 30 mph

inter·noise 2023
CHIBA,GREATER TOKYO 20-23 AUGUST
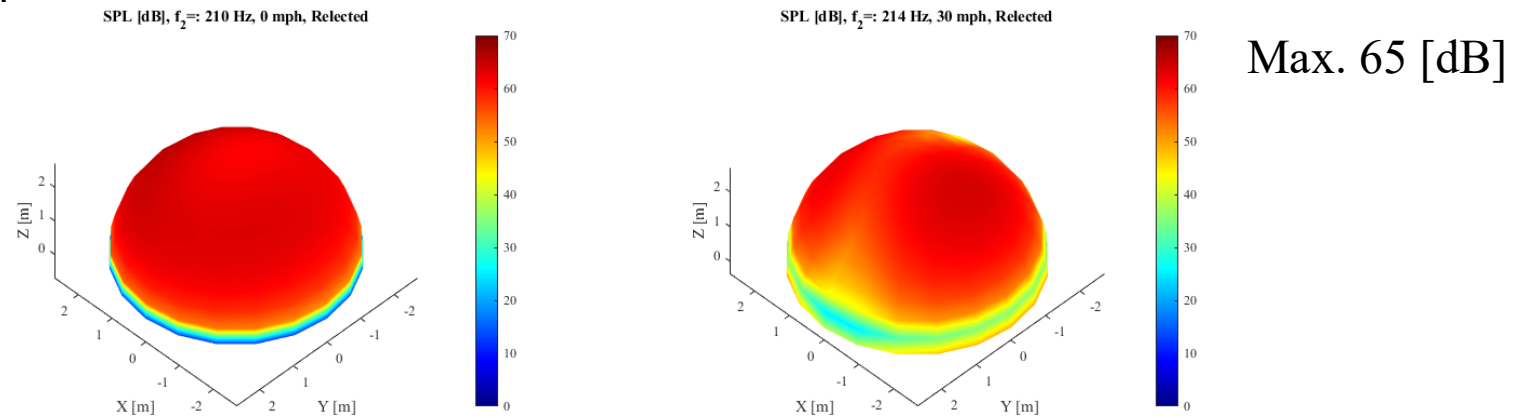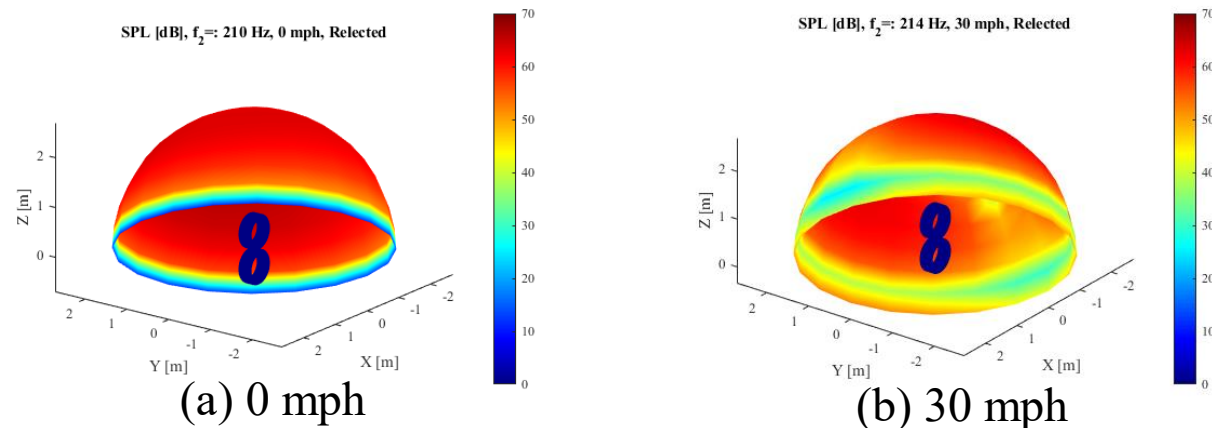
Future Work

1. **OBSI (On-Board Sound Intensity) testing** will be implemented to demonstrate the sound radiation pattern analyzed from the BEM analysis

2. **Commercial software** will also be deployed to obtain sound radiation fields in conjunction with vibrational analysis for a rolling tire

OBSI test (courtesy of AVEC INC.).

Actran (courtesy of MSC software).

Conclusions

1. **The previous FE simulation** that was used to predict spindle force **was extended here to a BEM analysis** to evaluate **a tire's sound radiation in a rolling condition** at two split frequencies relating to the **acoustic cavity mode**

2. **The OpenBEM code** created in Matlab was used to compute **the major matrices**, required in the **discretized Helmholtz equation**, with **surface meshes** imported from the FE model integrated with **a normal surface velocity** from the simulation results of Abaqus 2020

3. **A similar quadrupole pattern and SPL level** were obtained for the non-deformed tire under a static condition as compared to previous microphone measurements obtained by dropping a tire

4. The influence of reflecting ground on SPL level was studied such that **a doubling effect** of approximately 6 [dB] was observed **in the case of reflection** at zero speed as expected

5. **The evolution of SPL** at different rotation speeds up to 30 mph was analyzed where the SPL became the largest at 10 mph due to **the different strength of the coupling** between the cavity mode and adjacent tire's natural modes; but the maximum difference of SPL due to rotational speed does not exceed 3 [dB]

6. The effect of distance on the radiation pattern was found to retain a doubling effect: **6 [dB] increase as a distance is a halved**

7. **The entire sound mapping** over the hemisphere was created at two rotation speeds where rotation led to **asymmetric features** in sound radiation **as the tire rolls** over the ground and thus the normal surface velocity takes on a skewed shape

References

1. M. Parmar, B. Chandan, and M. Hari, "Stochastic simulation methodology accounting variability of key parameters affecting squeak and rattle performance", Proc. INTER-NOISE 20, I-INCE, Seoul, 2020, Section. 14.1, No. 145.

2. R. Bernhard et al., An introduction to tire/pavement noise of asphalt pavement, Virginia Asphalt Association, 2012.

3. Warped perception, GoPro Inside a Car Tire, 2020. (https://www.youtube.com/watch?v=rILyBg7ZjeI)

4. Kiran Patil, Jordan Schimmoeller, James Jagodinski, and Sterling McBride, Experimental observations in tire cavity resonance and interactions with periodic noise components, *Tire Science and Technology,* Vol. 23(1), pp. 2-10 (1995).

5. Vicente C. Henriquez and Peter M. Juhl, OpenBEM-An open source Boundary Element Method software in Acoustics. Proc. INTER-NOISE 10, 2010.

6. Won Hong Choi and J. Stuart Bolton, Force amplification at the wheel hub due to the split in the air-cavity mode for a rolling tire. Proc. NoiseCon 23.

7. Won Hong Choi and J. Stuart Bolton, Influence of the cavity mode on tire surface vibration. Proc. INTER-NOISE 11, pp. 2066-2073, 2011.

Acknowledgement

- Ford Motor Company – Financial support / Tire & wheel sample provider
- Matthew Black – Ford Program manager and logistical support
- Dean Smoll, Frank Lee and Jose Lopez Romero – Technical support at Purdue

Contact

Thank you!

Won Hong Choi
Ray W. Herrick Laboratories, Purdue University
177 S. Russell Street, West Lafayette IN 47907-2099
romeowonhong@gmail.com